Eur. Phys. J. B **46**, 15–19 (2005)
DOI: 10.1140/epjb/e2005-00233-1

THE EUROPEAN PHYSICAL JOURNAL B

Optimization of impurity profile for p-n-junction in heterostructures

E.L. Pankratov[1,a] and B. Spagnolo[2,b]

[1] Institute for Physics of Microstructures of RAS, GSP-105, Nizhny Novgorod, 603950, Russia
[2] INFM-CNR, and Dipartimento di Fisica e Tecnologie Relative, Group of Interdisciplinary Physics[c], Università di Palermo, Viale delle Scienze, pad. 18, 90128 Palermo, Italy

Received 10 November 2004 / Received in final form 2 May 2005
Published online 8 August 2005 – © EDP Sciences, Società Italiana di Fisica, Springer-Verlag 2005

Abstract. We analyze the dopant diffusion in p-n-junction in heterostructure, by solving the diffusion equation with space-varying diffusion coefficient. For a step-wise spatial distribution we find the optimum annealing time to decrease the p-n-junction thickness and to increase the homogeneity of impurity concentration in p or n regions.

PACS. 73.40.Kp III-V semiconductor-to-semiconductor contacts, p-n-junctions, and heterojunctions – 85.40.Ry Impurity doping, diffusion and ion implantation technology

1 Introduction

High performance and reliability of microelectronic devices and integrated circuits, recently attracted great interest [1–7]. To increase the performance of these devices it is important to decrease parasitic capacities, by decreasing the p-n-junction thickness, and at the same time to increase the homogeneity of impurity concentration. To obtain high current density in modern devices with lower dimensionality, in fact, it is crucial to have good interface profiles of dopant concentration. Different types of technology processes are used for production of p-n-junctions, such as short-time diffusion at high temperature and ion implantation usually in homogenous samples [1,4]. But it is necessary to develop new approaches to produce semiconductor devices with better characteristics: higher performance, smaller fluctuation of parameters, and decreasing of dimensions of elements of integrated circuits [8]. In this paper we present an approach to increase the performance of semiconductor devices by decreasing the parasitic capacitance of p-n-junction, by choosing the space dependence of diffusion coefficient and annealing time. We consider an epitaxial layer with thickness a and diffusion coefficient D_1, which has been sputtered on a substrate with thickness $(L-a)$, diffusion coefficient $D_2 < D_1$ and known type of conductivity (p or n) (see Fig. 1). Let us consider a dopant, which was infused into the epitaxial layer from the boundary $x = 0$. Its initial distribution is equal to $C(x,0) = f(x)$ and its spatial integral is normalized to unity $\int_0^L C(x,t)dx = 1$. The dopant gives a possibility to produce in the epitaxial layer the second type of conductivity (n or p). At the time $t = 0$ the temperature of the heterostructure (epitaxial layer-substrate) was increased rapidly with respect to typical time scale of the diffusion process t_a. This heating leads to diffusion of infused dopant in the heterostructure during time t_a. After the time interval t_a, the heterostructure was cooled rapidly with respect to time scale t_a and dopant diffusion was stopped. Here our aims are: (i) to reduce the parasitic capacitance of p-n-junction, by increasing the steepness of impurity concentration profile between p and n regions; (ii) to increase the homogeneity of impurity concentration in doped regions by optimization of distribution of infused dopant.

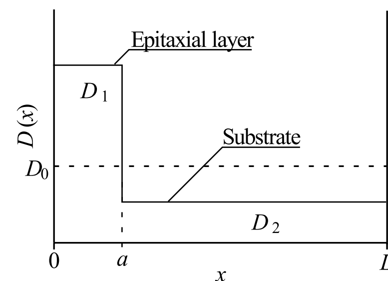

Fig. 1. Step-function space distribution of the diffusion coefficient in heterostructure.

2 Method of solution

Our starting point, to analyze the spatiotemporal distribution of dopant concentration in heterostructure, is the second Fick's law

$$\frac{\partial C(x,t)}{\partial t} = \frac{\partial}{\partial x}\left[D(x)\frac{\partial C(x,t)}{\partial x}\right] = -\frac{\partial G(x,t)}{\partial x}, \qquad (1)$$

[a] e-mail: `elp@ipm.sci-nnov.ru`
[b] e-mail: `spagnolo@unipa.it`
[c] `http://gip.dft.unipa.it`

Table 1. Values of parameter ϵ from references [9,10].

Heterostructure	Dopant	ϵ	Temperature
Si/Ge	As	0.075	700 °C
Si/Ge	B	0.09	700 °C
Si/Ge	P	0.12	800 °C
Si/Ge	As	0.23	800 °C

where $G(x,t)$ is the dopant flow. The initial and boundary conditions are: $C(x,0) = f(x)$ and $G(0,t) = G(L,t) = 0$. For analytical solution of diffusion equation (1) we use the following expression for the diffusion coefficient of heterostructure: $D(x) = D_0[1 + \epsilon g(x)]$, where $|g(x)| \leq 1$, D_0 is average value of diffusion coefficient, and $0 \leq \epsilon < 1$. Several examples of the parameter ϵ at different values of temperature are presented in Table 1.

The function $g(x)$, which corresponds to the profile of diffusion coefficient with two layers (see Fig. 1), is

$$g(x) = \begin{cases} 1, & 0 \leq \xi \leq \alpha \\ -\dfrac{\alpha}{1-\alpha}, & \alpha \leq \xi \leq 1, \end{cases} \tag{2}$$

where $\xi = x/L$ and $\alpha = a/L$. In previous investigations [1,3,11,12] the authors usually have calculated solutions of diffusion equation (1) for constant diffusion coefficient D_0 and for few types of initial and boundary conditions. Specifically absorbing boundaries, step or delta-functions as initial distribution of dopant concentration, and layered or exponential space distribution of diffusion coefficient have been considered.

First of all we solved equation (1) analytically. Analytical approximate solution has smaller exactness in comparison with numerical one. But it leads to more comprehensive results and helps to understand physical effects better. To solve analytically equation (1) with space varying diffusion coefficient $D(x)$, we use the expansion in power series of ϵ [13]

$$C(x,t) = \sum_{k=0}^{\infty} \epsilon^k C_k(x,t). \tag{3}$$

This approach will be, of course, useful for heterostructures with low values of parameter ϵ, as those shown in Table 1. By substitution of equation (3) into equation (1), and equating the coefficients with the same power of ϵ, we obtain the following system of equations for zero-order approximation of dopant concentration $C_0(x,t)$ and corrections to it $C_k(x,t)$ for $k \geq 1$

$$\begin{cases} \dfrac{\partial C_0(x,t)}{\partial t} = D_0 \dfrac{\partial^2 C_0(x,t)}{\partial x^2} \\ \dfrac{\partial C_k(x,t)}{\partial t} = D_0 \dfrac{\partial^2 C_k(x,t)}{\partial x^2} \\ \qquad + D_0 \dfrac{\partial}{\partial x}\left[g(x)\dfrac{\partial C_{k-1}(x,t)}{\partial x}\right], \quad k \geq 1. \end{cases} \tag{4}$$

From equation (3) we have the initial conditions for functions $C_k(x,t)$: $C_0(x,0) = f(x)$, $C_{k\geq 1}(x,0) = 0$, and the boundary conditions for functions $G_k(x,t)$: $G_{k\geq 1}(0,t) = G_{k\geq 1}(L,t) = 0$. By solving the first equation of the system (4), with above conditions, we obtain the zero-order approximation of dopant concentration

$$C_0(x,t) = \frac{1}{L} + \frac{2}{L}\sum_{n=1}^{\infty} \frac{F_n c_n(\xi) e_n(t)}{n}, \tag{5}$$

where $c_n(\xi) = n\cos(\pi n \xi)$, $e_n(t) = \exp\left[-n^2 t/\tau_1\right]$, $\tau_1 = L^2/(\pi^2 D_0)$, $F_n = n\int_0^1 f(\xi) c_n(\xi) d\xi$ and $\xi = x/L$. After substitution of the series $C_k(x,t) = \sum_{n=1}^{\infty} h_{nk}(t) n c_n(\xi)$ into the second and third equations of the system (4) we obtain the first and the second order corrections for the dopant concentration in the following form

$$\begin{cases} C_1(x,t) = -\dfrac{2}{L^2}\displaystyle\sum_{n=1}^{\infty} c_n(\xi) \sum_{m=1}^{\infty} m \dfrac{F_m e_{mn} G_{nm}}{nm}, \\ C_2(x,t) = \dfrac{2}{L^3}\displaystyle\sum_{n=1}^{\infty} c_n(\xi) \sum_{k=1}^{\infty} k^2 G_{nk} \\ \qquad \times \displaystyle\sum_{m=1}^{\infty} \dfrac{m F_m G_{km}}{km}\left[\dfrac{e_{mn}(t)}{nm} - \dfrac{e_{kn}(t)}{nk}\right], \end{cases} \tag{6}$$

where $nm = n^2 - m^2$, $G_n = \int_0^1 g(\nu) c_n(\nu) d\nu / n$, $e_{mn}(t) = e_m(t) - e_n(t)$, and $G_{ij} = G_{i-j} - G_{i+j}$ with $i,j = n,m,k$.

The expressions (5) and (6) for $C_0(x,t)$, $C_1(x,t)$ and $C_2(x,t)$ are valid for any profiles of diffusion coefficient $g(x)$ and any initial distribution $f(x)$. Now we consider a step-wise spatial distribution of the diffusion coefficient (see Eq. (2)) and initial condition $f(x) = \delta(x)$. After calculation of the coefficients F_n and G_n, we obtain from equations (5) and (6) the second order approximation of dopant concentration

$$\begin{aligned} C(x,t) \approx{}& \frac{1}{L} + \frac{2}{L}\sum_{n=1}^{\infty} c_n(\xi) e_n(t) - \frac{2\epsilon}{(1-\alpha)\pi L} \cdot \\ & \sum_{n=1}^{\infty} c_n(\xi) \sum_{m=1}^{\infty} \frac{m e_{mn}(t)}{nm}\left(s_{n-m} - s_{n+m}\right) \\ & + \frac{2\epsilon^2 \pi^{-2}}{(1-\alpha)^2 L}\sum_{n=1}^{\infty} c_n(\xi) \sum_{k=1}^{\infty} k^2 \left(s_{n-k} - s_{n+k}\right) \cdot \\ & \sum_{m=1}^{\infty} \frac{m}{km}\left(s_{k-m} - s_{k+m}\right)\left[\frac{e_{mn}(t)}{nm} - \frac{e_{kn}(t)}{nk}\right], \end{aligned} \tag{7}$$

where $s_n = sin\left[\pi n \alpha\right]/n$.

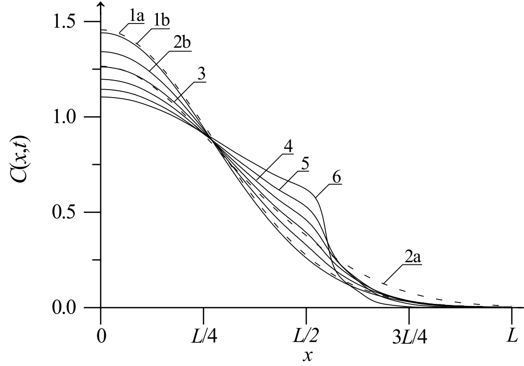

Fig. 2. Space distribution of impurity concentration at annealing time $t_a = \tau_1/20\pi^2$. Here $\alpha = 1/2$ and $C(x, 0) = \delta(x)$. Curves $1a$ and $1b$ correspond to $\epsilon = 0$; curves $2a$ and $2b$ corresponds to $\epsilon = 0.2$; curves $3 - 6$ correspond respectively to $\epsilon = 0.4, 0.6, 0.8, 0.999$. Dashed lines correspond to analytical solution of diffusion equation (see Eq. (7)), solid lines correspond to numerical solution of diffusion equation (1).

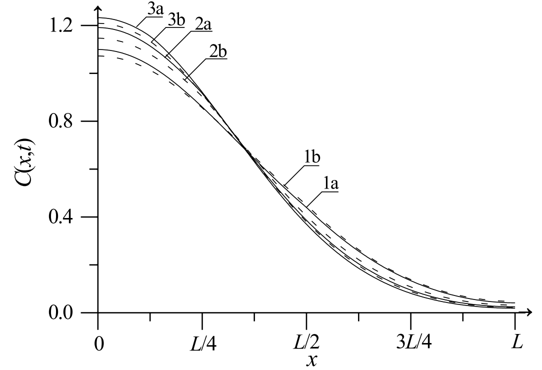

Fig. 3. Space distribution of impurity concentration at annealing time $t_a = \tau_1/20\pi^2$, for three values of the parameter α: $1/8, 1/4, 1/2$, corresponding respectively to curves $1 - 3$. The initial distribution is $C(x, 0) = \delta(x)$ and $\epsilon = 0.15$. Dashed lines correspond to analytical solution (Eq. (7)), solid lines correspond to numerical solution of diffusion equation (1).

3 Discussion

To optimize the annealing time in order to increase the steepness of impurity profile, for the considered case of heterostructure with two layers, we analyze the behaviors of the dopant concentration as a function of parameters ϵ and α, at different values of annealing time t_a. In Figure 2 we show the behavior of dopant concentration at fixed time t_a, for six values of the parameter ϵ and initial distribution $C(x, 0) = \delta(x)$. We see from this figure, that increasing the value of ϵ, i.e. increasing the difference between diffusion coefficients D_1 and D_2, leads to monotonous increase of steepness of impurity profile in substrate and increase of the homogeneity of impurity profile in doped region. This effect could be related to the semi-insulating property of the interface between layers of heterostructure. Figure 2 also shows that, increasing the parameter ϵ corresponds to increase the thickness of the region enriched by impurity (p or n type). The effective thickness of doped region can be determined by considering the following criterion, used for relaxation time [13,14]

$$\ell(t) = \frac{1}{C(0, t)} \int_0^L C(x, t)dx. \qquad (8)$$

Here $\ell(t)$ is the optimum thikness relate to the "ideal" impurity profile. By substituting equation (7) into equation (8) we obtain the second order approximation of the thickness of doped region of heterostructure, which we don't report here because its complicated expression. As an example for annealing time $t_a = \tau_1/20\pi^2$, after analytical calculation of the integrals and numerical summation, we obtain the following expression for the thickness of doped region

$$\ell \approx [0.396 + 0.775\alpha^{1.322}\epsilon - 0.6\alpha^{0.585}\epsilon^2]L. \qquad (9)$$

We analyze now the behavior of dopant concentration at different values of parameter α, for fixed values of parameter ϵ and annealing time t_a. Our analytical results, obtained from equation (7), and compared with numerical solution of equation (1) are shown in Figure 3. We can see that decreasing of parameter α, i.e. decreasing of the epitaxial layer thickness a, leads to monotonous increasing of homogeneity of impurity profile in epitaxial layer. The agreement between analytical and numerical results is very good. Our analytical approximations give correct results for values of parameter $\epsilon \leq 0.09$ (linear approximation of calculated results) and $\epsilon \leq 0.15$ (second-order approximation of calculated results), as in most heterostructures of practical interest. Thus, speed of convergence of our expansion (3) is enough good.

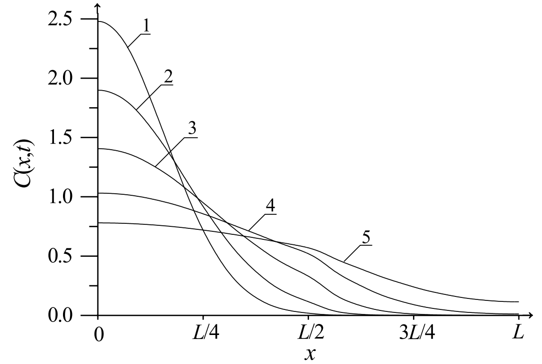

Fig. 4. Space distribution of impurity concentration at different values of annealing time t_a. Specifically the values t_a from top (1) to bottom (5) are: $\tau_1/16\pi^2$, $\tau_1/8\pi^2$, $\tau_1/4\pi^2$, $\tau_1/2\pi^2$, τ_1/π^2. The values of parameters are: $\epsilon = 0.5$, $\alpha = 1/2$, and initial distribution is $C(x, 0) = \delta(x)$.

Let us consider now space structure of dopant concentration at different values of annealing time t_a. These curves are shown in Figure 4, for initial distribution of concentration $C(x, 0) = \delta(x)$ and value of parameters: $\epsilon = 0.5$ and $\alpha = 1/2$. We see from this figure, that increasing of annealing time leads to increase the homogeneity of dopant concentration. Impurity profile, which has main practical interest, is almost constant in the area $0 \leq \xi \leq \alpha$, and

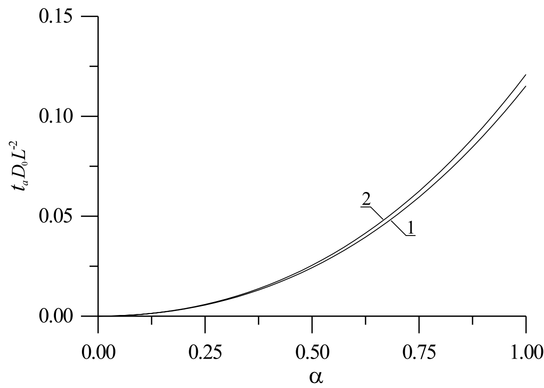

Fig. 5. Dependence of the normalized compromise annealing time on the parameter α, for fixed value of the parameter $\epsilon = 0.15$. Curve 1 – analytical approximation (Eq. (10)), curve 2 – numerical simulation (Eq. (1)).

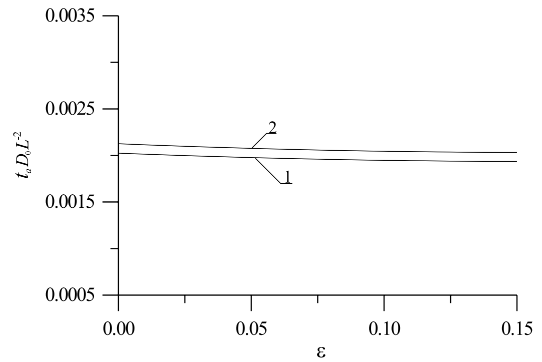

Fig. 6. Dependence of the normalized compromise annealing time on the parameter ϵ, for fixed value of the parameter $\alpha = 0.15$. Curve 1 – analytical approximation (Eq. (10)), curve 2 – numerical simulation (Eq. (1)).

rapidly decreases in the other region. Thus, it is necessary to determine such an annealing time, which corresponds to a compromise between homogeneity of impurity profile in epitaxial layer and decreasing of impurity concentration in substrate (compromise annealing time). For determination of the optimal annealing time we use two criteria.

For the first criterion we introduce the function $\beta(x, t_a) = C(x, t_a)/C(0, t_a)$, which can be considered as heterogeneity coefficient and characterizes decreasing of impurity concentration space dependence from the maximal value at time t_a. We estimate the compromise annealing time from following condition: $\beta(a, t_a) = 1/\sqrt{2}$. This corresponds to decreasing of the impurity concentration of $3dB$ at the epitaxial layer thickness in such a profile, formed during annealing time t_a. Inserting equation (7) into the expression $\beta(x = a, t_a) = 1/\sqrt{2}$, after numerical summation, we obtain the second-order approximation of compromise annealing time

$$t_a \approx [0.36 - 0.2\alpha^{1/3}\epsilon + 5.814\alpha^{1.17}\epsilon^2]\alpha^2\tau_1\pi^2, \tag{10}$$

where the first term is the zero-order approximation, which is related to the case of constant diffusion coefficient. We note that this term is approximately twice the annealing time obtained in the case $\epsilon = 1$ (see Refs. [13, 14]). In Figures 5 and 6 we show the behaviors of optimum annealing time as a function of parameters α and ϵ respectively. We see that the agreement between analytical approximation (curves 1 in the figures) and direct simulation of equation (1) is quite good. Moreover we observe that decreasing parameter α, or increasing parameter ϵ, leads to decrease the annealing time at compromise.

The second way to estimate the compromise annealing time is to minimize the following expression (i.e. to optimize this time)

$$U = \int_0^L \{C(x, t) - C_f[\theta(x) - \theta(x - \ell_f)]\}^2 \, dx, \tag{11}$$

in order to obtain the homogenous distribution impurity concentration in epitaxial layer. Here $C(x, t) = C_f[\theta(x) - \theta(x - \ell_f)]$ is the ideal impurity profile, C_f and ℓ_f are constant, $\theta(x)$ is the step-function

$$\theta(x) = \begin{cases} 0, & x < 0 \\ 1/2, & x = 0 \\ 1, & x > 0. \end{cases}$$

After minimization of equation (11), by mean-square error technique, and using equation (3) we obtain the system of equations for the zero-order approximation of the annealing time t_{a0} and for corrections t_{ak} (for $k \geq 1$)

$$\begin{cases} \int_0^L C_0(x, t_a) \dfrac{\partial C_0(x, t_a)}{\partial t_a} dx = C_f \int_0^{\ell_f} \dfrac{\partial C_0(x, t_a)}{\partial t_a} dx \\ \int_0^L C_{k\geq 1}(x, t_a) \dfrac{\partial C_{k\geq 1}(x, t_a)}{\partial t_a} dx = 0. \end{cases} \tag{12}$$

Calculation of the compromise annealing time based on the system (12) gives us approximately the same result obtained by using the function $\beta(x, t)$:

$$t_a \approx [0.434 - 0.306\alpha^{0.4}\epsilon + 5.3\alpha\epsilon^2]\alpha^2\tau_1/\pi^2.$$

Last criterion is qualitatively shown in Figure 7, where we report different impurity profiles corresponding to increasing annealing time. From this figure we see that the optimum annealing time is that related to impurity profile 3.

4 Conclusions

We analyzed the dopant dynamics by solving the diffusion equation with diffusion equation varying in space. We derived, for heterostructures of practical interest, an analytical approximate solution, which is valid for any spatial

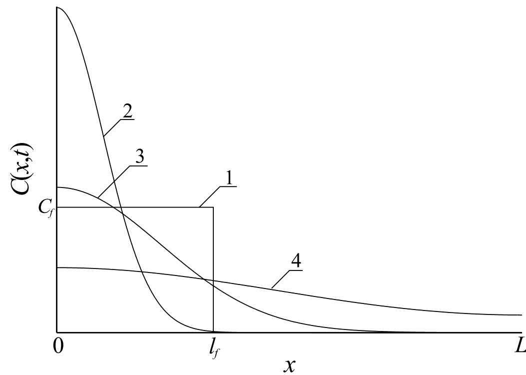

Fig. 7. Curve 1 - ideal impurity profile, curves 2-4 – real impurity profiles at different increasing annealing times (from 2 to 4).

profile of diffusion coefficient and for any initial distribution. For step-wise spatial distribution we obtained the effective thickness of doped region and the optimal annealing time, which corresponds to maximal compromise between increasing of homogeneity of impurity concentration in doped region of heterostructure and increasing of steepness of p-n-junction.

By increasing the difference between diffusion coefficients of layers of heterostructure and by correct selecting the annealing time, we obtain an almost homogeneous distribution of donors or acceptors in doped region and an increasing of the steepness profile in un-doped region of semiconductor structure. Our approach enables us to consider additional terms in expansion of equation (3) to improve the optimization of impurity profile for p-n junction in heterostructures, paying attention to the complexity of the analytical expression obtained with respect to a direct simulation of the diffusion equation.

This work has been supported by MIUR, INFM-CNR, INTAS (project 2001-0450), by the grant of Scientific Schools of Russia (project SS-1729.2003.2) and by RFBR (project 05-02-17340-a).

References

1. A.B. Grebene *Bipolar and MOS analogous integrated circuit design* (New York, John Wiley and Sons, 1983)
2. T. Oka, K. Ouchi, K. Mochizuki, T. Nakamura, Solid State Electronics **41**, 1611 (1997)
3. I. Zutic, Y. Fabian, S. Das Sarma, Phys. Rev. B **64**, 121201 (2001)
4. S.T. Sisianu, T.S. Sisianu, S.K. Railean, Semiconductors **36**, 581 (2002)
5. W.M. Chen, I.A. Buyanova, A.V. Buyanov et al., Phys. Rev. Lett. **77**, 2734 (1996)
6. P. Laitinen, A. Strohm, A. Neiminen et al., Phys. Rev. Lett. **89**, 085902 (2002)
7. P. Laitinen, Riihimäki, Räisänen et al., Phys. Rev. B **68**, 155209 (2003)
8. T. Oka, K. Hirata, H. Suzuki et al., Int. J. of High Speed Electronics and System, **11**, 115 (2001)
9. R.N. Ghoshtagore, Phys. Rev. B **3**, 397 (1971); R.N. Ghoshtagore, Phys. Rev. B **3**, 2507 (1971)
10. P.M. Fahey, P.B. Griffin, J.D. Plummer, Rev. Mod. Phys. **61**, 289 (1989)
11. B.A. Zon, S.B. Ledovskiy, A.N. Likholet, Technical Physics **45**, 419 (2000)
12. Y.Y. Shan, P. Asoka-Kumar, K.G. Lynn, Phys. Rev. B **54**, 1982 (1996)
13. A.A. Dubkov, A.A. Mal'tsev, E.L. Pankratov, Technical Physics **47**, 1359 (2002)
14. A.N. Malakhov, E.L. Pankratov, Radiophysics and Quantum Electronics **44**, 339 (2001)